

## CHAPTER 1

# MODELING RUNUP WITH DEPTH INTEGRATED EQUATION MODELS

G. Pedersen

*Mechanics Division, Department of Mathematics, University of Oslo  
E-mail: geirkp@math.uio.no*

This survey starts with a sketch of long wave theory, reflecting some of its diversity. Next, general aspects of runup on sloping beaches are briefly discussed in the scope of long waves, including important analytical solutions, breaking criteria, significance of non-hydrostatic effects and experiments. Then the literature on numerical modeling of runup is reviewed. The models are loosely organized into classes and then described chronologically within each class. Primarily, we refer models that are published in international journals, while matter from the vast number of proceedings and internal reports are mentioned occasionally. Moreover, we highlight the verification of the numerical methods by comparison to analytical solutions or experiments. Applications to real tsunami or storm surge events are, with a few exceptions, not included.

### 1. Introduction

Comprehension of wave runup on beaches is essential for prediction of beach erosion and coastal impact of tsunamis and storm surges. This is one reason for the lasting attention that runup topics have received in the literature of hydrodynamics and coastal engineering. Moreover, this complicated, yet commonplace phenomenon, that can be observed at every beach with incident swells or wind waves, pose mathematical and conceptual challenges that appeal to many scientists. Wave runup also inherits similarities to other important phenomena in hydrodynamics, such as “green water” (wave overtopping on vessels), slamming and interaction between the ocean pycnocline and bathymetry.

As for many other wave phenomena, long wave theory has been crucial for our understanding of wave runup on beaches and derivation of closed form solutions supporting this understanding. Also numerical models for

large scale ocean waves in general, such as tides, storm surges and tsunamis, have traditionally been based on shallow water theory, due to the simplicity and efficiency of this formulation. Certainly, more general models are in progress, also for runup on beaches<sup>23–25,43,50,51,70,109</sup>, but do still involve heavy computations. For instance, most fair sized three-dimensional wave problems are still dependent on approximate methods, such as long wave theory. In fact, even an idealized, two-dimensional simulation modeling the propagation of a tsunami wave or swell from deep water, through shoaling/surf and to runup on a shore will often border on the limits of models based on the Navier-Stokes equations or full potential theory. Therefore, for many applications we must rely on long wave models also in the years to come.

In the context of depth integrated equations, the moving shoreline on a beach is in some respects similar to a free water surface that is deformed by waves; the flow field is confined by a time dependent boundary with a position that is unknown *a priori*. Furthermore, in both cases the surface excursions correspond to motion of material particles with gravity as restoring force. However, there are important differences. In runup the medium is “thinning” toward the shoreline, resulting in a singularity in the governing equations, though not in the physically relevant solutions. In addition, wave breaking and topographical effects are often important for the near-shore flow. If we look beyond the long wave (depth-integrated) description, other aspects appear, such as the dynamics of a contact point between a free surface and a rigid no-slip boundary, boundary layers, and effects of bottom porosity. These are presumably most important on laboratory scale and are anyway outside the scope of the present article.

An early review on long wave runup is found in Meyer and Taylor (1972)<sup>67</sup>. The predecessors to the “The Third International Workshop On Long-Wave Runup Models”, leading to this volume, also initiated articles summarizing aspects of runup research<sup>53,113</sup>. Among the contributions are overviews of finite difference and element methods for tsunamis, that also address long wave runup<sup>32,105</sup>.

This review is meant to provide a brief and updated status on long wave runup models, with an inclination toward applicability of the different long wave approximations. We do not include related themes such as runup on vertical walls, edge waves, rip currents, and impact problems. Moreover, we focus on the principal aspects of physics and modeling rather than case studies of real events of tsunamis and storm surges. Wave breaking is the subject of Chapter 2 (by LeVeque and George) in this volume<sup>48</sup>. Still, for

completeness, models with breaking, as well as theory and experiments, will be discussed briefly herein.

We start with a short presentation of relevant parts of long wave theory. Then the runup phenomenon is discussed with selected analytic solutions and experiments, before the diversity of models in the literature will be summarized. No complete assessment of the various methods will be attempted, but documentation of performance through comparison with analytic solutions, experiments, other models and grid refinement will generally be emphasized. Significance of physical processes like wave dispersion will also be addressed when appropriate.

## 2. Long Wave Equations

Following standard conventions we employ a typical depth  $d$  and a wavelength  $L$  as vertical and horizontal length scales, respectively. The choice of  $L$ , in particular, is ambiguous and it may also correspond to other lengths than that of a wave. Identifying the time scale  $t_c = L/\sqrt{gd}$ , where  $g$  is the acceleration of gravity, and the dimensionless amplitude,  $\epsilon$ , we define  $\epsilon L/t_c$ ,  $\epsilon d/t_c$  and  $\epsilon d$ , respectively, as scales for horizontal velocity, vertical velocity and surface elevation. When we instead refer to dimensional quantities they are marked by a star. Different long wave equations can be obtained through perturbation expansions in  $\mu \equiv d/L$  and  $\epsilon$  and may then be classified according to which orders of these parameters that are retained in the equations. Omission of all  $\mu$  terms yields the nonlinear shallow water (NLSW) equations, while retaining second-order in  $\mu$  yields Boussinesq type equations that are available in a series of varieties<sup>61,79,110</sup>. Long wave approximations prescribe simple vertical structures for the field variables. In NLSW theory, the horizontal velocity is vertically uniform and the pressure hydrostatic. Therefore, the vertical coordinate,  $z$ , vanishes from the equations. When  $O(\mu^2)$  terms are retained there are vertical variations in the horizontal velocity. Still, the explicit appearance of  $z$  is removed from the continuity and momentum equations by integration. Hence, we denote them as “depth integrated equations”. The spatial dimension of the partial differential equations is then reduced by one. Furthermore, the nonlinear free surface appears only through nonlinear coefficients. These features make long wave formulations well suited for numerical solution. Regardless of the mathematical reduction of dimension, we will still refer to problems as two- or three-dimensional according to the physical configuration.

The order of a long wave equation is reflected in the dispersion characteristics. According to full potential theory the dispersion relation of a

linear, sinusoidal wave reads (depth:  $h = 1$ )

$$c^2 = \frac{1}{k\mu} \tanh(\mu k) = 1 - \frac{1}{3}(\mu k)^2 + \frac{2}{15}(\mu k)^4 + \dots, \quad (1)$$

where  $c$  is the phase speed and  $k$  is the wave number. Shallow water theory only reproduces the first term on the right hand, while traditional Boussinesq equations yield the first two. However, as we will see below, different formulations valid to  $O(\mu^2)$  give different dispersion properties. They may even reproduce the  $O(\mu^4)$  term in (1) correctly or display an extended validity range.

### 2.1. Boussinesq Theory

During the last fifteen years fully nonlinear Boussinesq type equations with improved dispersion properties have been put to work in computer models. Following Hsiao *et al.* (2002)<sup>29</sup> we write a set of fully nonlinear Boussinesq equations on the form

$$\eta_t = -\nabla \cdot [(h + \epsilon\eta)(\mathbf{v} + \mu^2\mathbf{M})] + O(\mu^4), \quad (2)$$

$$\begin{aligned} \mathbf{v}_t + \frac{\epsilon}{2}\nabla(\mathbf{v}^2) = & -\nabla\eta - \mu^2 \left[ \frac{1}{2}z_\alpha^2\nabla\nabla \cdot \mathbf{v}_t + z_\alpha\nabla\nabla \cdot (h\mathbf{v}_t) \right] \\ & + \epsilon\mu^2\nabla(D_1 + \epsilon D_2 + \epsilon^2 D_3) + O(\mu^4) + \mathbf{N} + \mathbf{E}, \end{aligned} \quad (3)$$

with

$$\mathbf{M} = \left[ \frac{1}{2}z_\alpha^2 - \frac{1}{6}(h^2 - \epsilon h\eta + \epsilon^2\eta^2) \right] \nabla\nabla \cdot \mathbf{v} + \left[ z_\alpha + \frac{1}{2}(h - \epsilon\eta) \right] \nabla\nabla \cdot (h\mathbf{v}),$$

$$D_1 = \eta\nabla \cdot (h\mathbf{v}_t) - \frac{1}{2}z_\alpha^2\mathbf{v} \cdot \nabla\nabla\mathbf{v} - z_\alpha\mathbf{v} \cdot \nabla\nabla \cdot (h\mathbf{v}) - \frac{1}{2}(\nabla \cdot (h\mathbf{v}))^2,$$

$$D_2 = \frac{1}{2}\eta^2\nabla \cdot \mathbf{v}_t + \eta\mathbf{v}\nabla\nabla \cdot (h\mathbf{v}) - \eta\nabla \cdot (h\mathbf{v})\nabla \cdot \mathbf{v},$$

$$D_3 = \frac{1}{2}\eta^2 [\mathbf{v} \cdot \nabla\nabla \cdot \mathbf{v} - (\nabla \cdot \mathbf{v})^2],$$

and where the index  $t$  denotes temporal differentiation,  $h$  is the equilibrium depth,  $\eta$  is the surface elevation,  $\mathbf{v}$  is the horizontal velocity evaluated at  $z = z_\alpha(x, y)$  and  $\nabla$  is the horizontal component of the gradient operator. The heuristic terms  $\mathbf{N}$  and  $\mathbf{E}$  in the momentum equation (3) represent bottom drag and artificial diffusion and will be discussed below. This particular form of the leading dispersion ( $\epsilon^0\mu^2$ ) term was discussed and tested by Nwogu (1993)<sup>71</sup>, while additional nonlinearity was added by Wei *et al.*

(1995)<sup>107</sup>. A similar formulation, with the velocity potential as primary unknown instead of the velocity, is found in Chen and Liu (1995)<sup>7</sup>. Applying transformations and deletion of various higher order terms to the set (2) and (3), we may reproduce a number of other Boussinesq type equations from the literature<sup>42,71,107</sup>. As pointed out in the references<sup>107</sup> weakly nonlinear versions, in the sense that some or all  $O(\epsilon\mu^2)$  terms are omitted, may sometimes yield nonzero volume flux at the shore. This should in particular be avoided for runup simulations.

When  $h$  is constant and  $\epsilon \rightarrow 0$  Boussinesq equations on the form (2,3) yield  $c^2$  as a rational function of  $\mu^2 k^2$ . For  $z_\alpha = (\sqrt{1/5} - 1)h$  this expression reproduces the first three terms in the expansion (1), while  $z_\alpha = -0.531h$  yields a particularly favorable dispersion relation over an extended range of wave numbers. (see Fig. 1). With  $z_\alpha = (\sqrt{1/3} - 1)h$ , the velocity  $\mathbf{v}$  differs from the depth averaged velocity ( $\bar{\mathbf{v}}$ ) by  $O(\epsilon\mu^2)$ , only. If we then delete all  $O(\epsilon\mu^2)$  terms in (2) and (3) we retrieve the traditional Boussinesq equations for constant depth. These possess a dispersion relation that is clearly inferior to the optimal version of (2,3) (Fig. 1). In general, the form of the volume flux in (2) implies<sup>a</sup>  $\bar{\mathbf{v}} = \mathbf{v} + \mu^2 \mathbf{M}$ . Differentiating this relation with respect to time, inserting the resulting expression for  $\mathbf{v}_t$  in (3), and invoking  $\mathbf{v} = \bar{\mathbf{v}} + O(\mu^2)$  in nonlinear and dispersive terms we obtain the standard Boussinesq equations that inherit errors of order  $\epsilon\mu^2, \mu^4$

$$\eta_t = -\nabla \cdot [(h + \epsilon\eta)\bar{\mathbf{v}}], \tag{4}$$

$$\begin{aligned} \bar{\mathbf{v}}_t + \frac{\epsilon}{2} \nabla(\bar{\mathbf{v}}^2) = & -\nabla\eta + \mu^2 \left[ \frac{h}{2} \nabla\nabla \cdot (h\bar{\mathbf{v}}_t) - \frac{h^2}{6} \nabla\nabla \cdot \bar{\mathbf{v}}_t \right] \\ & + O(\epsilon\mu^2, \mu^4) + \mathbf{N} + \mathbf{E}. \end{aligned} \tag{5}$$

This set has been used much in numerical simulations and for the first time by Peregrine (1967)<sup>78</sup> for the shoaling of a solitary wave. We will subsequently refer to formulations like (4,5) as “standard” Boussinesq equations, whereas those with more accurate dispersion properties, such as (2,3) with  $z_\alpha = -0.531h$ , will be denoted as “improved”.

Further information on, and extensions of, higher order long wave equations are found in a number of papers in the literature<sup>16,58–61</sup>. However, progress has primarily been made with respect to higher order nonlinearity

---

<sup>a</sup>To reproduce  $\bar{\mathbf{v}}$  from  $\mathbf{v}$  in non-constant depth we would have to employ a time dependent  $z_\alpha$ .

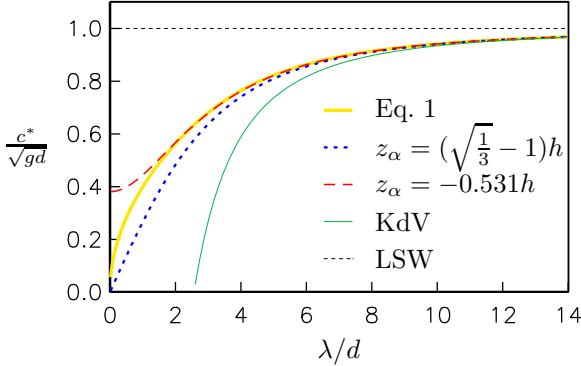


Fig. 1. The phase speed as function of wavelength for long wave equations compared to that of the fully inviscid set. The curve for the Korteweg-deVries (KdV) equation is included for comparison.

and dispersion during propagation in mildly varying bathymetries. Corresponding improvement has not yet been reported for a rapidly varying bottom. The shoreline, with its mathematical singularity and abrupt change of wave characteristics, as discussed below Eq. (7), may hardly be regarded as belonging to a region of mild slope. Hence, while the higher order Boussinesq formulations are of great value in finite depths, it remains to be seen what may be locally achieved in runup on a sloping beach. In fact, as will be discussed subsequently, even the significance of leading order dispersion is debatable in the vicinity of the shoreline.

## 2.2. Shallow Water Equations

Deletion of all  $O(\mu^2)$  terms simplifies (2,3) to the NLSW equations. The pressure gradient in the momentum equation then becomes  $\nabla\eta$ , corresponding to hydrostatic pressure. As a consequence the horizontal velocity becomes independent of  $z$ . The NLSW equations lack the important effect of wave dispersion and may lead to erroneous results for long term propagation, even if the waves are long compared to the depth<sup>79</sup>. However, they are still quite a reasonable option for surf zone dynamics and are, by far, the most commonly used framework for runup calculations, as well as tsunami and storm surge models. Also the NLSW equations may be reformulated in different ways. For modeling shocks (bores), in particular, it is important to recast the momentum equations into a conservative form. When  $F$  and  $B$  are omitted we may write the  $x$ -component as

$$(Hu)_t + (\epsilon Hu^2 + \frac{1}{2}H^2)_x + \epsilon(Huv)_y = Hh_x, \quad (6)$$

where subscripts indicate partial derivation,  $H = h + \epsilon\eta$ , and  $u$  and  $v$  are the velocity components in the  $x$ - and  $y$ -directions, respectively. Naturally, a corresponding equation applies to the  $y$ -direction. We observe that the right hand side is a momentum source due to a sloping bottom. Often the depth integrated fluxes are used as primary unknowns instead of the velocities. This may cause difficulties during runup, since velocities are needed for the propagation of the shoreline and the relation between fluxes and velocities may be poorly defined when  $H \rightarrow 0$ .

A popular transformation of the NLSW equations is obtained through introduction of characteristics. For plane waves the characteristic equations become

$$\beta_t^\pm + (\epsilon u \pm c)\beta_x^\pm = h_x, \quad \text{where} \quad \beta^\pm = \epsilon u \pm 2c, \quad c = \sqrt{h + \epsilon\eta}. \quad (7)$$

Characteristics played an important role in the early analytic work on runup of breaking waves<sup>41,87</sup> and are used in some numerical runup models as well<sup>72,101,102</sup>. In these references the technique is extended to two horizontal directions by operator splitting<sup>102</sup> or a partial characteristic description<sup>72</sup>. At the shoreline  $c$  becomes zero and both the characteristic equations and variables in (7) coalesce. Alternative equations or extrapolation must then be employed in a numeric model. Moreover, as long as  $\partial(h + \epsilon\eta)/\partial x$  is nonzero at the shoreline, the spatial derivative of  $c$  is non-finite, which is a challenge from a computational point of view. Still, as demonstrated in the references runup can be treated accurately and efficiently by (7).

If the two-dimensional NLSW equations are linearized, we may eliminate the velocity to obtain a very simple equation

$$\eta_{tt} - (h\eta_x)_x = 0. \quad (8)$$

It might seem counter-intuitive for such an apparently nonlinear phenomenon, but linear equations work surprisingly well on a number of runup problems.

### 2.3. Lagrangian Coordinates and ALE Formulations

Problems involving material boundaries that are moving make application of Lagrangian coordinates tempting. In the limit  $\mu \rightarrow 0$  the horizontal velocity is uniform in depth and it displays only a weak vertical variation for small  $\mu$ . A Lagrangian description may thus be based on material columns of water for the NLSW equations and averaged columns for Boussinesq equations. A common choice for coordinates is the initial positions of the columns, but every mapping of these are feasible and do not lead to

more complicated equations. The transformation between Eulerian and Lagrangian coordinates,  $(a, b)$ , expresses that the latter are constant for a fluid particle;  $a_t + \mathbf{v} \cdot \nabla a = 0$  and  $b_t + \mathbf{v} \cdot \nabla b = 0$ . Applying this transformation to equations of the form (2,3), with a value of  $z_\alpha$  corresponding to depth averaged velocities, we arrive at equations for  $x$ ,  $y$  and  $\eta$  according to

$$(h + \epsilon\eta) \frac{\partial(x, y)}{\partial(a, b)} = F(a, b), \quad (9)$$

$$\frac{\partial(x, y)}{\partial(a, b)} \frac{x_{tt}}{\epsilon} = -\frac{\partial(\eta, y)}{\partial(a, b)} + O(\mu^2), \quad \frac{\partial(x, y)}{\partial(a, b)} \frac{y_{tt}}{\epsilon} = -\frac{\partial(x, \eta)}{\partial(a, b)} + O(\mu^2), \quad (10)$$

where only the NLSW terms are spelled out and the Jacobi determinants are defined according to

$$\frac{\partial(x, y)}{\partial(a, b)} = \frac{\partial x}{\partial a} \frac{\partial y}{\partial b} - \frac{\partial x}{\partial b} \frac{\partial y}{\partial a}.$$

We note that time derivatives of positions are of order  $\epsilon$  such that the ordering of (10) is consistent. Both a standard form of the Boussinesq equations<sup>115</sup> and a fully nonlinear version for plane waves<sup>34,75</sup> are available. Comparing (9,10) to the Eulerian counterpart we observe that the convective terms have vanished and that ungracious Jacobi determinants have appeared. Moreover, the continuity equation has been integrated once in time to directly express the volume conservation in a material fluid column, with  $F$  representing volume per area in the  $a, b$  plane.

For wave propagation in one horizontal direction the choice of marker coordinates is unproblematic, but non-rectangular two-dimensional horizontal domains have to be resolved with curvilinear grids or finite elements. For runup the Lagrangian description has the major advantage that the shoreline is located at temporally fixed values of  $a$  and  $b$ ; the computational domain is independent of time. As a bonus this sometimes extends also to piston type wave paddles that may be cumbersome to incorporate in Eulerian models.

To the knowledge of the author no Lagrangian version of improved Boussinesq equations akin to (2,3) have been reported. Presumably, there are no principal difficulties in the transformation, but it will result in very lengthy expressions.

The fully Lagrangian description, where particles are traced throughout the fluid, is in fact an over-treatment of the moving boundary problem. We need only to follow the boundary particles and may thus employ a wider class of transformations, that may be referred to as Arbitrary Lagrangian

Eulerian (ALE). There is a large diversity with respect to selection of coordinates and dependent variables. In the simplest case with runup of plane waves an obvious choice is a time dependent stretching of the spatial coordinate in accordance with the shoreline motion. For simple three-dimensional geometries, typically having a single, moderately curved shoreline, a similar stretching with an along-beach variation may be employed<sup>72,84</sup>. With more complex geometries the transformation to time dependent curvilinear coordinates may be found by optimizing with respect to local refinement, variability and skewness of the grid (measured in the physical plane), while fixed grid-boundaries (in the coordinate plane) are constrained to follow the shoreline(s)<sup>88</sup>.

In three-dimensional runup problems the ALE technique may be formulated more robust with respect to interior grid deformations due to currents than the purely Lagrangian ones. However, both traditional Lagrangian and ALE methods are susceptible to grid deformation when large inundation takes place in complex geometries. In addition bathymetric data must be interpolated at each time step in numerical simulations.

#### 2.4. The Shoreline

We observe that the linear wave equation (8) has a singularity for  $h = 0$ . Provided that the gradient of  $h$  is finite at the shoreline both singular and regular solutions exist. The simplest example is that of a linear standing wave with frequency  $\omega$  on an inclined plane defined by  $h = \alpha x$ . The regular solution, that has physical significance, then reads

$$\eta = AJ_0(2\omega\sqrt{\alpha x}) \cos(\omega t + \delta), \quad (11)$$

where  $A$ ,  $\delta$  are constants and  $J_0$  is the Bessel function of zero order that may be expanded in even powers of its argument. For the singular solution of (8) we have  $\eta \sim \ln(x)$  for small  $x$ , while the horizontal velocity has a pole of order 1. As a consequence there is a volume source at the singularity. Hence, runup models that do not conserve volume at the shoreline should be checked extra carefully for accuracy and spurious behavior. The mathematical structure with regular and singular solutions carries over to nonlinear equations as well as full potential theory<sup>33</sup> and is further discussed in a long wave context by Meyer<sup>65,66</sup> and others.

For nonlinear equations the shoreline is signified by  $H = h + \epsilon\eta = 0$ . In addition the position of the shoreline must be traced. We confine the discussion to two dimensions and assume that the shoreline always

consists of the same material particle. The shoreline position,  $x = \xi$ , then moves according to  $\frac{d\xi}{dt} = u(\xi, t)$ . In Lagrangian description this is only an instance of the unknown  $x(a, t)$ , but in Eulerian models the equation for  $\xi$  must somehow be integrated. This is often achieved implicitly by filling and emptying of grid cells. For very steep and breaking waves, outside the long wave regime, the shore may not always correspond the same particle(s). Moreover, the waterline is affected both by bottom roughness, viscosity and capillary effects. The latter are generally more significant on the laboratory scale than for real tsunamis and storm surges, say. One should always bear this in mind when models are calibrated against experiments.

### 2.5. Additional Effects

For waves propagating across oceans the rotation of the Earth must be taken into account as the Coriolis force. However, the local runup dynamics on a shore is hardly influenced by such effects and further discussion of this topic is thus omitted.

Bottom friction is often included in long wave models as a square of the velocity. A common form is

$$\mathbf{N} = -\frac{\epsilon K}{\mu H} |\mathbf{v}| \mathbf{v}, \quad (12)$$

where  $K$  is an empiric constant. Unfortunately, much of the systematic empiric data for bottom friction stem from steady channel flow and may not be relevant for the thin and rapidly changing fluid layers in runup. Moreover, there is no consensus concerning the use of drag terms like (12). Zelt and Raichlen (1991)<sup>116</sup> calibrated the formula against experiments<sup>94</sup> and then settled for  $K = 5 \times 10^{-5}$ . Comparing with the same dataset, Lynett *et al.* (2002)<sup>57</sup> suggested a value an order of 100 larger. We also observe that the above formula in principle becomes singular at the shoreline.

Bores may be included in the NLSW description as discontinuities in the velocity and the surface elevation. In numeric models these may be reproduced by special shock capturing schemes, generally applying approximate solvers of Riemann problems (evolution of step distributions). Alternatives that give finite width bores and may be used also with Boussinesq type equations are the roller model<sup>62</sup> or inclusion of a diffusion term,  $\mathbf{E}$ , in (3). For plane wave this term typically reads

$$E^{(x)} = H^{-1}(\nu(Hu)_x)_x. \quad (13)$$

Such terms have often been included to stabilize numerical models, under cover of being a physical eddy viscosity effect. With a constant  $\nu$  (13) is quite inefficient as a tool for controlling wave breaking. Zelt (1991)<sup>114</sup> made  $\nu$  dependent on the velocity gradient in a similar term.  $\nu$  was zero until the gradient reached a threshold value and then increased with the gradient beyond this. The critical value of the velocity gradient was related to the highest stable solitary wave, which has an amplitude 0.78 times the depth<sup>b</sup>. Kennedy *et al.*<sup>42</sup> expressed  $\nu$  by  $\eta_t$  and pursued the idea further by including an explicit time relaxation for  $\nu$  after activation of the diffusion. This method has been demonstrated to reproduce bores from experiments very well<sup>42,57</sup>. However, as pointed out in a reference<sup>56</sup>, this procedure may not recognize a nearly stationary bore on a current, like the one that often forms during drawdown at beaches.

## 2.6. Numerical Modeling of Long Waves

There are numerous papers on numerical solution of NLSW and standard Boussinesq equations in general. Finite difference (FD) techniques dominate, but quite a number of finite element (FE) methods are reported as well. In traditional ocean and tsunami models the NLSW equations are often solved by explicit methods and discretized on staggered grids<sup>64</sup> (see Fig. 2), denoted as C-grid, B-grid etc. Many FD models employ discretization in finite volumes with fluxes defined at the interfaces to assure conservation of mass and momentum. This is particularly important for shock propagation models. Under-resolved models inherit a strong artificial dispersion that occasionally may mimic true dispersion. However, this cannot be accounted upon as a reliable feature and should be avoided. Grid sensitivity tests are crucial in this context.

Boussinesq equations must be simulated by implicit methods and lead to more CPU-time consuming models than the NLSW counterparts. As compared to standard Boussinesq formulations the additional higher order derivatives of the formulation (2,3) lead to extended computational molecules and more difficult boundary conditions. This, in addition to the lengthy expressions, render the implementation of this more general formulation somewhat deterring. However, two FD codes for numerical solution of this set may be downloaded from the Internet, namely the FUNWAVE<sup>44,45</sup>

---

<sup>b</sup>Recent investigations indicate that cross-wise instability appears at smaller amplitudes<sup>40</sup>.

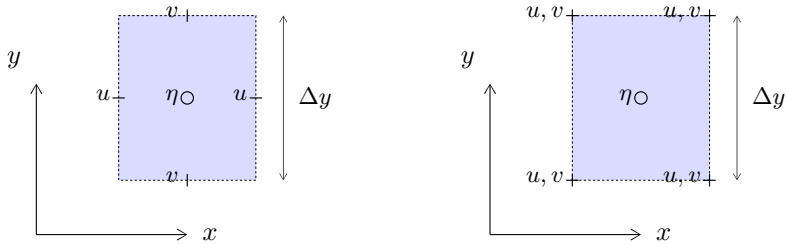


Fig. 2. Left panel: The C-grid that defines a basic configuration for mass conserving FD methods. It is used also for many Navier-Stokes models with  $\eta$  replaced by pressure. Right panel: The less used B-grid. This is well suited for representation of deformation, as needed in Lagrangian models.  $u$  and  $v$  are the velocity components in the  $x$ - and  $y$ -directions, respectively.

and COULWAVE<sup>56</sup> models. These contain a number of features, including runup facilities. Both models employ fourth order (five point) and second order differences for the  $O(\mu^0)$  and the  $O(\mu^2)$  terms, respectively, combined with higher order time integration. As a consequence, the leading dispersion in the wave celerity, namely the second term in (1), is kept clean of discretization errors, which is a natural objective for numerical solution of enhanced Boussinesq equations.

Solution of (2,3) by a finite element method is reported by Woo and Liu<sup>108</sup>, where the problem with higher order spatial derivatives is resolved by introduction of extra dependent variables.

### 3. The Runup Phenomenon; Reference Solutions and Experiments

Runup is generally part of a more complete problem, where some incident wave is present in finite depth. This then undergoes shoaling and amplification, and may turn into a bore, before it reaches the beach and starts to run up (or down), often as a long and thin tongue that is retarded by gravity. The withdrawal phase is then characterized by the run-down of a thin layer of fluid, often with a strong bore, oriented onshore, evolving at the toe. This whole sequence involves many stages and different physical mechanisms. There is a rich literature on both shoaling and surf-zone dynamics that is outside the scope of this paper. Turbulence and sedimentation in the swash zone<sup>12,54,83,85</sup> are directly related to runup, but are also side issues in the present context.

### 3.1. The Non-Breaking Regime

The closed form solutions for runup are mostly associated with hydrostatic ( $\mu \rightarrow 0$ ) theory. We will discuss some aspects of these solutions with reference to a wave in a generic wave tank, as depicted in Fig. 3, with an incident wave characterized by a length  $\lambda$  and amplitude  $A$ . The quantity  $\ell$  is the propagation distance in constant depth, for instance the distance from a wave maker to the slope. In the limit  $\mu \rightarrow 0$  the equations are independent of the choice for the scaling factor  $L$ , introduced at the start of Sec. 2. Rescaling with the length of the slope,  $d \cot \theta$ , as  $L$  we then realize that the solution of the problem in Fig. 3 is governed by the parameters  $\epsilon = A/d$ ,  $\kappa = L/\lambda$  and  $\ell/\lambda$ .

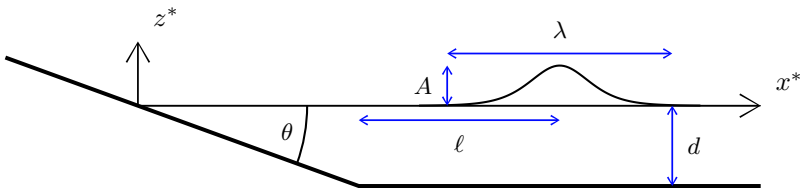


Fig. 3. Definition sketch of generic wave tank.

In 1958 Carrier and Greenspan<sup>5</sup> presented their much celebrated nonlinear, analytic solutions of the NLSW equations for runup on an inclined plane. They invoked a transformation that in dimensionless form reads

$$\sigma = 4\sqrt{x + \epsilon\eta}, \quad \lambda = 2(t - \epsilon u), \quad u = \frac{\phi_\sigma}{\sigma}, \quad \eta = -\frac{\phi_\sigma}{4} - \epsilon \frac{u^2}{2}. \quad (14)$$

The potential,  $\phi$ , then solves the linear wave equation

$$\phi_{\lambda\lambda} - (\sigma\phi_\sigma)_\sigma = 0.$$

Among their explicit solutions were the nonlinear generalization of (11), the standing wave, as well as an initial value problem for runup. We will subsequently refer to these solutions as  $CG-s^5$  and  $CG-i^5$ , respectively. A kind of breaking, in the sense that  $\eta$  becomes multivalued as function of  $x$ , is also contained in the standing wave solution. A major problem with the transformation is the specification of an incident wave. Carrier (1966)<sup>4</sup> suggested the coupling of the nonlinear solution with a linear outer solution, possibly including dispersion and a general bottom profile, through linear

patching conditions. This idea has later been exploited by others, among which the work of Synolakis (1987)<sup>94</sup> has made most impact. Before going into details we will remark on some general properties of this approach. Since the transformed equations, as well as far-field and patching are linear, the solutions in  $\sigma$  and  $\lambda$  equal linear solutions in the physical plane with  $\sigma^2/16$  and  $\lambda/2$  substituted for  $x$  and  $t$ , respectively. Nonlinearity enters first through the transformation (14) back to the physical variables. When  $u$  is zero, as at the point of maximum excursion of the shoreline, the nonlinearity also disappears from this transformation. Hence, the maximum runup height for the combined linear/non-linear theory will be as for a purely linear one. Moreover,  $\ell$  only gives a time shift when the constant depth region is governed by the LSW equations. For the wave tank problem in Fig. 3 the maximum runup height then becomes

$$R = AF(\kappa), \quad (15)$$

where  $F$  is a function depending on the actual shape of the incident wave (an example is given below).

Solitary waves<sup>68</sup> are much used in theoretical runup investigations, even though they are more rarely seen in nature. They have permanent form, finite width and are easy to create in a laboratory. To leading order in  $\mu$  and  $\epsilon$  the solitary wave solution in dimensional form reads

$$\eta^* = A \operatorname{Sec}^2(k(x^* - ct^*)), \quad k = \frac{1}{d} \sqrt{\frac{3A}{4d}}, \quad c = \sqrt{gd} \left(1 + \frac{1}{2} \frac{A}{d}\right). \quad (16)$$

In reality solitary waves are both nonlinear and dispersive, but the expression (16) may anyhow be used as initial condition in the combined linear/nonlinear calculations described above. Synolakis<sup>94</sup> applied Fourier transforms to find a simple asymptotic formula for the maximum runup height of solitary waves. Defining  $\lambda$  as  $1/k$  we make the identification  $\kappa = kd \cot \theta$  and write the formula on the form (15)

$$R = 3.042A\kappa^{\frac{1}{2}} = 2.831A(\cot \theta)^{\frac{1}{2}} \left(\frac{A}{d}\right)^{\frac{1}{4}} \quad \text{for } \kappa \rightarrow \infty. \quad (17)$$

When  $A$  and  $k$  in (16) are regarded as independent we observe that the runup decreases with the wavelength. This is general feature of the present theory that is found also for periodic waves. There are two main sources of errors in (17), namely the asymptotic assumption and the lack of dispersion on the slope. To check the effect of the first we may simply find  $R$  by solving (8) numerically. Application of a five point centered difference scheme, with

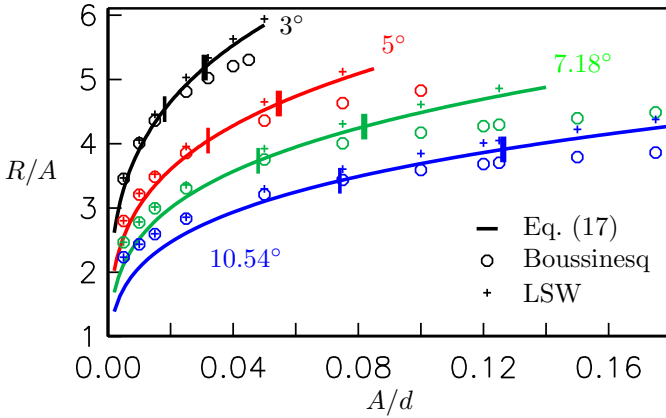


Fig. 4. Shallow water and Boussinesq predictions for maximum runup heights of solitary waves for different beach inclinations as indicated on the curves. The thick and thin columns represent breaking limits, (20), during runup and drawdown, respectively.

the closest node half a grid increment from the shore to implement the condition of zero flux, makes this a trivial task. The results are subsequently shown in Fig. 4.

The effect of dispersion on solitary wave runup is frequently overlooked when NLSW models are compared to experiments or dispersive models are compared with analytic NLSW solutions. This makes the model assessments imprecise, with a negative bias concerning model performance. We may employ optics to obtain a simple estimate on the variation of dispersion with depth. Assuming that the period is unchanged during shoaling, we find that the wavelength is reduced as  $h^{-\frac{1}{2}}$  and the relative size of the leading dispersion term in the wave celerity vanishes proportional to  $h$  near shore. However, this result will not be valid in the proximity of the shore and nonlinear effects will lead to steepening of the wave front, which in turn enhance dispersion. Therefore, we resort to employment of a Lagrangian Boussinesq type model<sup>34,76</sup> (Sec. 4.1), that was readily at hand for the author. Converged results of both the LSW and Boussinesq models are compared to (17) in Fig. 4, that also contains the breaking criteria as given in Eq. (20). Shallow water theory over-predicts runup slightly for the larger  $A/d$ , but is surprisingly close to the Boussinesq theory even beyond the hydrostatic breaking limit. For large  $\theta$  and small  $A/d$ , meaning small  $\kappa$ , the numeric solutions coincide, while the asymptotic formula (17) deviates. Hence, we clearly observe the asymptotic nature of the closed form solution

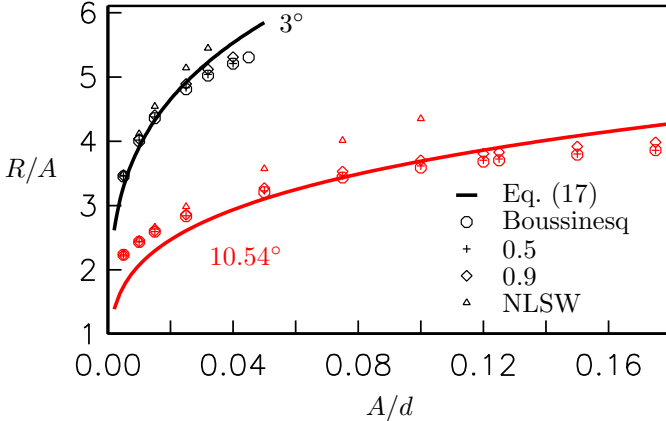


Fig. 5. Maximum runup heights for solitary waves. Results from combined Boussinesq/NLSW theory are marked by the transition depth  $h(a_c)$  at equilibrium.

and that the agreement is good down to  $\kappa = 1$ , say, that corresponds to  $R/A \approx 3.04$  in the figure.

We have also performed some numerical experiments to unravel where dispersion effects are important. To this end we introduce a variable  $\mu(a)$ , where  $a$  corresponds to the initial distance from the shore (Sec. 2.3). In deep water  $\mu$  has its proper value, but over an interval  $(a_c, 1.1 \times a_c)$  it is reduced to zero. As shown in Fig. 5, omission of dispersion over half the slope does not influence the maximum runup. Even if the hydrostatic region is increased to nearly the whole slope, the change in  $R$  is very small, though breaking occurs for a smaller  $A$ . The largest error occur when also the uniform depth region is made non-dispersive (data marked NLSW in the figure). This deviation depends strongly on  $\ell$  that in the present simulation is chosen as  $\ell = -\ln(0.00025)d/\sqrt{3A/d}$ , which corresponds to an initial  $\eta^*$  equal to  $A/1000$  at the start of the slope. In Fig. 6 we have compared the particle acceleration in the Boussinesq model to the contribution from the hydrostatic part of the pressure gradient, given by  $\partial\eta/\partial x$ , for a moderately steep incident wave. In finite depth there is a mild influence of the non-hydrostatic pressure (right panel). When the wave have just reached the shore the surface has an inclination of  $36^\circ$ , which is steeper than an extreme (maximum amplitude) Stokes or solitary wave. Still, the non-hydrostatic part of the pressure gradient is noticeable only in a small region close to the shore.

Naturally, here we have merely scratched the surface concerning applicability of long wave theories. Still, it is indicated that for non-breaking waves

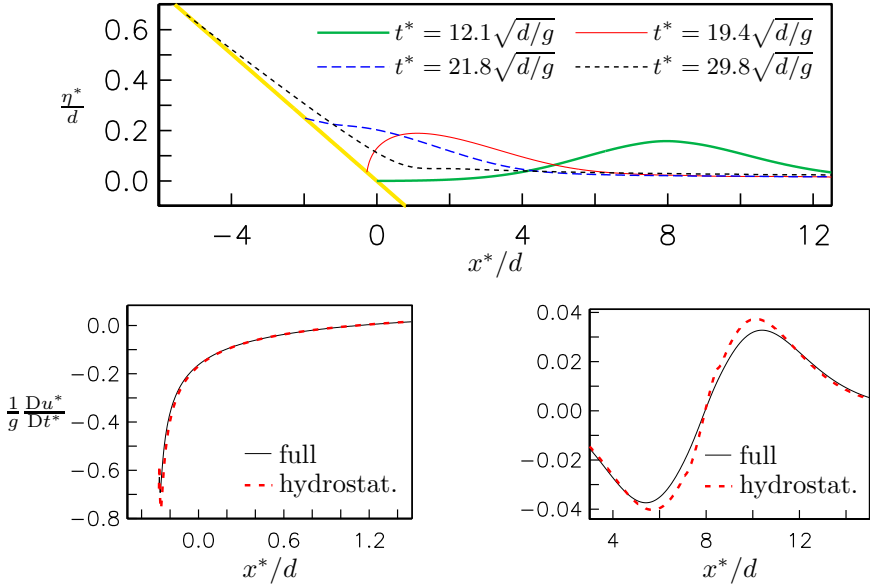


Fig. 6. Runup of a solitary wave with  $A/d = 0.15$  and  $\theta = 7.18^\circ$ . Upper panel: Surfaces for the incident wave, an early stage in runup, an intermediate stage and maximum runup. Lower panels: Comparison of the full acceleration to the part that stems from the hydrostatic pressure gradient. Left: Vicinity of beach for the second time (thin solid line in upper panel). Right: The incident wave (rightmost wave profile in upper panel).

the NLSW equation will often do for the near-shore region and runup. An equally important lesson is that dispersion should not readily be ignored for the constant depth propagation in simulations of wave tank experiments.

There are other analytic runup solutions that deserve mentioning. Some are related to those above, but involve different initial conditions, slides or modified geometries<sup>3,6,39,49,74,77,92,95,97,103</sup>.

Another class of solutions contains the eigenoscillations in basins of parabolic bottom shapes that are summarized by Thacker<sup>100</sup>. There exist closed form solutions of the NLSW equations for the two lowest eigenmodes. In the first mode the whole fluid body moves back and forth in a uniform horizontal motion, driven by a uniform pressure gradient associated with a linear surface. Setting  $d$  equal to the maximum depth, identifying the half-width of the of equilibrium surface with  $L$  and choosing  $\epsilon d$  as the amplitude of the lowest harmonic in  $\eta^*$ , we obtain simple formulas for the 2D case

$$\eta = \cos(\sqrt{2}t)x - \frac{\epsilon}{4} \cos^2(\sqrt{2}t), \quad u = -\frac{1}{\sqrt{2}} \sin(\sqrt{2}t). \quad (18)$$

It is noteworthy that the eigenfrequency is independent of the amplitude. The second mode inherits a linear spatial variation of the velocity and a second order polynomial for the surface. The first eigenmode is much used for comparison with and validation of numerical methods. However, this may be a deceiving test due to the extremely simple spatial structure of the flow that is reproduced exactly by many methods that may give large discretization errors under other circumstances. It will serve best for validation of code or performance check of crude shoreline approximations. The second mode has somewhat better perspectives for assessment of runup models, but is used less often.

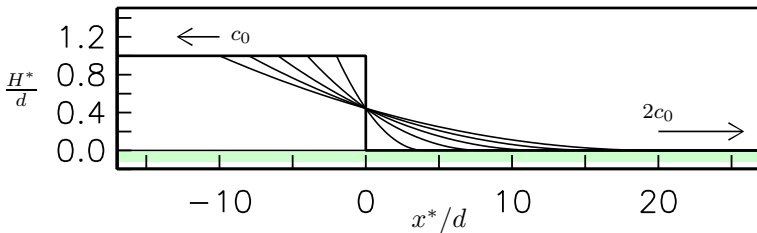


Fig. 7. The dambreak solution according to (19). Surfaces are depicted for  $t^* = 0, \Delta t^* \dots$ , where  $\Delta t^* = 2d/c_0$ .

An important analytic solution of the shallow water equations is that of dam-break<sup>93</sup>, where a mound of water, usually step sized, is released from rest at an horizontal plane. The initial acceleration distribution and early development of the flow pattern are also extended to full potential theory<sup>63</sup>. Even though the initial water front is vertical, a smooth thin tongue will evolve. Assuming an initial condition with fluid height  $d$  for  $x^* < 0$  and a dry bed for  $x^* > 0$  we obtain a self-similar dilution wave from the NLSW equations. For  $-c_0 t^* < x^* < 2c_0 t^*$  the solution reads (see Fig. 7)

$$H^* = \frac{d}{9} \left( \frac{x^*}{c_0 t^*} - 2 \right)^2, \quad u^* = \frac{2}{3} \left( c_0 + \frac{x^*}{t^*} \right), \quad (19)$$

where  $H^*$  is the total water depth and  $c_0 = \sqrt{gd}$  is the long wave speed in depth  $d$ . Dam-break is a standard test case for Navier-Stokes models, and is quite common for long wave solvers as well. NLSW models may strive to reproduce the break at the limit to quiescent water, the huge accelerations for small times, and perhaps the thin and rapidly moving fluid tip. Otherwise, the solution (19) share the weakness of the eigenoscillations

in parabolic basins concerning verification of NLSW models. The spatial structure of the flow is too simple to put many techniques to a proper test.

### 3.2. Transition to Breaking

Relevant overviews and background information on wave breaking may be found in, for instance, Cokelet<sup>11</sup>, Peregrine<sup>80</sup> and, Synolakis and Skjelbreia<sup>96</sup>.

From the NLSW solutions of the preceding section we also have breaking criteria for solitary waves during runup and drawdown on a plane beach on the form

$$\frac{A}{d} < C(\tan \theta)^{\frac{10}{9}} \quad \text{or} \quad \kappa^{\frac{5}{2}} \frac{A}{d} < \left(\frac{3}{4}\right)^{\frac{5}{4}} C^{\frac{9}{4}}. \quad (20)$$

For runup the constant  $C = 0.82$  is reported<sup>94</sup>, while  $C = 0.48$  is obtained for drawdown<sup>15</sup>. These findings are consistent with the commonly observed feature that waves break more easily during withdrawal. The breaking limits are depicted in Fig. 4. From the figure we observe that the breaking criterion for runup is too strict compared to the Boussinesq results. This is as expected since dispersion slow down the steepening during shoaling. Grilli *et al.*<sup>24</sup> have investigated breaking of solitary waves on a beach by a boundary integral method for full potential theory. The reference recognized two breaking regimes: one with breaking before the shoreline, or on-shore plunging, and an intermediate regime with a (nearly) vertical front at, and a little beyond the equilibrium shoreline, which transforms into a smooth swash without any appreciable plunging or spilling. Applying curve fitting to the breaking/no-breaking domains in the  $A, \theta$  plane, approximate criteria were presented as

$$\frac{A}{d} = B \tan^2 \theta, \quad (21)$$

where  $B = 16.9$  and  $B = 25.7$  correspond to the lower boundaries of the intermediate and strongly breaking regimes, respectively. The criterion (21) is generally much more relaxed than (20). However, it must be remarked that the definition of breaking is ambiguous and that (21) is based on few data points, in particular for small  $A/d$  and  $\theta$  where (20) is most likely to apply. Experiments<sup>34</sup> have confirmed the existence of the intermediate zone and even revealed waves that were overhanging at the shore, but still did not proceed to breaking. Instead, the steepening process was reversed and a smooth swash emerged from the toe of the wave.

Plunging breakers are outside the long wave regime, but fully developed bores may be crudely presented as discontinuities in shallow water solutions. This theme is treated in Chapter 2 (by LeVeque and George) in this volume and we will merely attach a few comments on the runup aspects. The most remarkable feature for bore runup<sup>28,41,67,87</sup> is that the bore collapses rapidly at the shoreline, giving birth to a long thin runup tongue with a height that is proportional to the square of the distance from the instantaneous shoreline. The swash is dominated by gravity and the runup trajectory becomes a parabola in the  $x, t$  plane. This transition from a steep incident wave to a swash is closely related to dam-break<sup>34,67,81</sup> (see Fig. 7). The runup of steep non-breaking waves and finite width bores are quite similar to that of the idealized bore solution; a steep front is transformed into a thin swash zone, where gravity often dominates over pressure effects<sup>34,114</sup>. Moreover, there are large accelerations and velocities in the early phases of runup, when the steep front vanishes. Small timing errors in experiments or models may lead to large deviations temporarily, while quantities like runup height and overall pattern is less influenced. This may cause an under-rating of model performance. The occurrence of a very thin runup layer that even may vanish as the square of the distance from the tip, seemingly argue against the application of a linear onshore extrapolation of the surface that is employed in some models. Even more so, perhaps, since the rundown phase display even thinner layers. On the other hand, bottom roughness, finite width bores and turbulence will modify the swash zone dynamics. Since, in addition, the feedback of a thin swash to the main body of fluid may be small, it is quite likely that surface extrapolation may be acceptable also in such cases.

### 3.3. Experiments

There is only a limited number of published experimental investigations that are commonly used for assessment of theoretic models. Hall and Watts (1953)<sup>26</sup> measured runup heights of solitary waves for different amplitudes and beach inclinations. Synolakis (1987)<sup>94</sup> published runup heights of breaking and non-breaking solitary waves on a 1.0 in 19.85 slope and amplitudes in the range  $0.004 < A/d < 0.6$ . In addition, data from a set of wave gauges, on and off the beach, were combined to rather complete surface elevations at different times. These surfaces have been valuable for validation of numerical models, in particular for the breaking cases. One such data-set is displayed in Fig. 10.

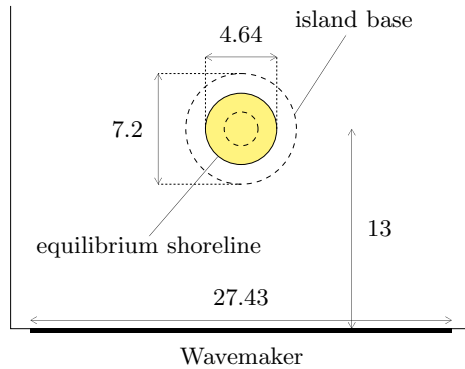


Fig. 8. Definition sketch of conical island experiment, with scales in meter. The outer dashed circle is the base of the island, the fully drawn circle is the equilibrium shoreline when  $d = 0.32\text{m}$ .

Briggs *et al.* (1995)<sup>2</sup> investigated runup on a conical island, with slope 1 in 4, situated on plane bed of equilibrium depth,  $d$ , 0.32m or 0.42m (Figs. 8 and 9). This experiment was inspired by observed runup patterns at a rounded island for the Flores tsunami in 1992<sup>112</sup>. Among the incident waves were plane solitary waves with amplitudes a little short of  $A/d = 0.05, 0.1, 0.2$ . Wave heights were measured at different offshore wave gauges and special gauges at the sloping bottom provided coarse digital series of inundation and withdrawal around the island. The experiments are also described in detail by Liu *et al.* (1995)<sup>52</sup> with the first numeric simulations on this problem. It is noteworthy that the breaking criterion (21) states that no solitary wave will break during runup on a plane 1 in 4 beach. Solitary waves of amplitude 0.2, or less, may then come close to breaking<sup>c</sup> only during withdrawal or due to three-dimensional effects. The criterion (20) yields  $A/d = 0.175$ , but the slope is too steep and the solitary wave too high (and short) for shallow water theory to apply. The most remarkable feature of the measured runup was a pronounced local maximum at the rear of the island, due to interaction of waves coming from either side. It is noteworthy that linear theories<sup>14,38</sup> reproduce the experiments very well, save for the lee side and then particularly the local maximum for the intermediate amplitude  $A/d = 0.1$ . The conical island experiment was used as a benchmark problem for the Second workshop on long wave runup<sup>113</sup>.

<sup>c</sup>The Boussinesq model<sup>34</sup> employed in Sec. 3.1 indicates breaking during retreat for  $A/d = 0.2$ , but not for the smaller amplitudes.

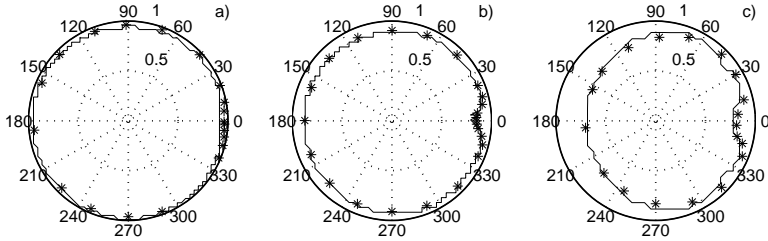


Fig. 9. Measured<sup>2</sup> (stars) runup on conical island with recent simulations by Lynett *et al.*<sup>57</sup> (lines). (a):  $A/d = 0.05$ , (b):  $A/d = 0.1$ , (c):  $A/d = 0.2$ . Reproduced from Lynett *et al.* by courtesy of the Coastal Engineering.

There are other experimental investigations of runup that, so far, are less used for verification of long wave models<sup>34,49,50,67,69,111</sup>.

#### 4. Runup Models

We may recognize at least three key problems in runup modeling:

- (1) The shoreline position is unknown *a priori*, it must be determined as a part of the solution procedure. The computational domain must somehow be adjusted to the shoreline motion.
- (2) The singularity at the shoreline means that there do exist singular solutions of the PDEs that may be excited by numeric errors.
- (3) It is difficult to find a sufficient number of accurate boundary conditions, in contrast to, for instance, the symmetry condition at a vertical wall. In finite difference methods one sided representations are generally required at shoreline. These may be implemented directly or indirectly by fictitious points combined with extrapolation. Common consequences are that the order of accuracy of the numerical method is reduced at the waterline and a production of noise that must be controlled by filtering or dissipation.

In view of these points the performance of runup models should be carefully assessed. Results should be compared to the analytic solutions or experiments on runup, or at least compared to computational results obtained independently. In addition, grid dependence in the solution, which always can be investigated, should be reported. It is surprising and disappointing how seldom the latter is found in the literature.

Some of the literature that addresses moving shorelines is focused on storm surges and tides. Such applications involve smaller gradients and longer time scales than runup of tsunamis, or swells, and are thus less challenging. The contributions of this kind often omit both testing and detailed descriptions of shoreline dynamics. Hence, it is difficult to evaluate the potential of such published methods concerning runup of steeper waves.

In the subsequent review, priority will be given to articles where validation in at least one of the above fashions is documented. The methods are grouped in two: those that remove the time dependence of the computational domain by a transformation, and those formulated on a fixed grid, possibly with some auxiliary nodes at the shoreline. Both groups contain finite difference as well as finite element methods. The reader should always bear in mind that the referenced articles vary in style and objective. Hence, when we are enabled to refer discussions on errors and shortcomings from a particular work this may equally well reflect quality and open-mindedness, on the authors side, as inferior model performance relative to other publications.

#### 4.1. *Transformed Domain Methods*

Application of a Lagrangian, or an arbitrary Eulerian-Lagrangian (ALE), description generally eliminates the tracing of an *a priori* unknown shoreline (point 1 above). Several runup models of this kind have been reported, even though they are in minority relative to the Eulerian counterparts.

An early discussion of runup and Lagrangian coordinates is given by Shuto (1967)<sup>89</sup>, but for the linear shallow water equations only. Hence, the potential of the Lagrangian description was not really exploited. Later Goto (1979)<sup>20</sup> and Goto and Shuto (1980, 1983)<sup>21,22</sup> compared 2D numeric results with linear solutions and the nonlinear standing wave solution  $CG-s^5$ . The description of the method was sketchy, but the agreement with the analytic solution was very good and markedly better than for some early Eulerian models. In 1983 Pedersen and Gjevik<sup>75</sup> applied Lagrangian coordinates to a 2D Boussinesq set with standard linear dispersion properties. Employing finite differences on a staggered grid the authors reproduced analytical solutions<sup>92</sup> accurately. Computed runup of non-breaking solitary waves were compared to experiments, with good agreement for moderately steep slopes. The model has later been revisited and improved by Jensen *et al.* (2003)<sup>34</sup>, who also discussed the significance of different  $O(\epsilon\mu^2)$  terms in the runup. A 3D Lagrangian FD model was reported by Johnsgard and

Pedersen (1997)<sup>37</sup> and Johnsgard (1999)<sup>36</sup> with applications to runup and wave generation by sub-aerial slides in idealized lake geometries. The model was based on a B-grid and verified by extensive grid refinement and comparison with  $CG-s^5$  and oscillations in a parabolic basin<sup>100</sup>.

Lynch and Gray (1980)<sup>55</sup> described a finite element technique with time dependent shape functions and a grid that could be adapted to a moving shoreline. However, their model was not tested on any standard problem. The first runup model that inherited both three-dimensionality and dispersion was published by Zelt and Raichlen in 1990<sup>115</sup>. They employed a finite element technique with a partition in quadrilaterals in the Lagrangian coordinates. One appealing feature of this kind of formulation is the so-called natural boundary condition for the shoreline. After reproducing  $CG-s^5$  accurately the authors applied the model to the response of an idealized harbour to incident swells. Their equations were similar to the standard Boussinesq equations, apart from some extra error terms of order  $\epsilon^2$  (see Sec. 2) that appeared for curved beach profiles. This minor fault was eliminated in the succeeding work<sup>114</sup>, where wave inundation of a horizontal shelf were modeled with a bottom friction term, giving good agreement with experiments. In a subsequent paper<sup>114</sup> Zelt included wave breaking by means of a diffusion (Sec. 2.5) dependent on the local wave steepness, or, rather, the compression rate of the Lagrangian water columns. Computations were compared with non-breaking ( $A/d = 0.04$ ) and breaking ( $A/d = 0.28$ ) solitary wave runup experiments<sup>94</sup>. Excellent agreement was observed for non-breaking runup, while there were discrepancies for breaking waves. In particular, a spurious, nearly vertical front persisted during inland excursion, which presumably was due to the diffusion term. Comparison was also made between Boussinesq, as well as NLSW, simulations and experiments<sup>19</sup> of solitary wave runup on a steep ( $\theta \approx 20^\circ$ ) slope. It is noteworthy that the Boussinesq results reproduced the experiments much closer (see discussion in Sec. 5). Later another Lagrangian FE method for the NLSW equations was reported by Petera and Nassehi (1996)<sup>82</sup>. Unfortunately, little documentation on the runup was given and there is no evidence of any improvement over the FE technique described above.

In two dimensions, the fluid domain can be mapped onto a fixed interval through a time dependent, but spatially uniform, coordinate stretching in accordance with the waterline motion. An example was given for the NLSW equations by Johns (1982)<sup>35</sup> who employed a staggered grid and linear extrapolation of  $\eta$  to obtain the shoreline position. A numeric solution showed fairly good agreement with an  $CG-s^5$  solution with a very small

amplitude. A similar technique was reported by Takeda (1984)<sup>99</sup>, who used a semi-characteristic method to reduce the need for one-sided approximations at the shore. Good agreement with  $CG-s^5$  was found for runup, while a somewhat degraded performance was observed for drawdown. The paper contains a general discussion on employment of asymmetric difference equations at the shore, but no model test that could support any firm conclusion was included. The approach of Johns<sup>35</sup> was generalized to three dimensions by Shi and Sun (1995)<sup>88</sup> who invoked an orthogonal transformation and then a C-grid discretization on a fixed coordinate domain that was composed of rectangles. The technique was applied to a real storm surge inundation. The large deformation of the grid imposed by the adaptation to a real geometry clearly called for grid-refinement studies, but none were presented.

In Özkan-Haller and Kirby (1997)<sup>72</sup>, the NLSW equations were rewritten in a partial characteristic form and solved on a transformed domain of rectangular shape by spectral collocation. Chebyshev polynomials and trigonometric functions were used for the cross- and along-shore directions, respectively. The  $CG-s^5$  solution was reproduced with high accuracy and the method was then applied to edge-wave instability. An advantage over fully Lagrangian techniques is that strong shear currents may be included without grid distortion. Recently, Prasad and Svendsen (2003)<sup>84</sup> have employed a similar transformation with a finite difference technique for the NLSW equations and obtained close agreement with both  $CG-s^5$  and  $CG-i^5$ . The authors also presented a FD technique on a fixed grid, where they went to some length in describing the shoreline accurately by carefully discretized boundary conditions. Also this technique displayed good results, but was markedly more prone to shoreline fluctuations than the transformation method and displayed a slower convergence according to grid refinement tests. Zhou *et al.* (2004)<sup>117</sup> make the same simple transformation as Johns<sup>35</sup> for the two-dimensional problem. The NLSW equations are then solved by a mesh-less technique, utilizing smooth shape functions and collocation. The paper is brief and only dam-break is presented as verification.

#### 4.2. Fixed Grid Methods

In a fixed grid the key problem is to include/exempt points and allot proper values to field variables at the boundary. For finite difference methods this is most commonly attempted by more or less ingenious extrapolation schemes. A number of such are reviewed in Imamura (1996)<sup>32</sup>. Balzano (1998)<sup>1</sup> tested

a series of NLSW methods for tidal flooding, mainly based on the C-grid, on a small amplitude second eigenmode in a parabolic basin<sup>100</sup>. To a greater or lesser extent all techniques gave near-shore fluctuations. However, the degree of nonlinearity was too small to allow any inference on the general runup performance of the models.

Apart from simulations of flooding based on linear theory<sup>86</sup>, the first proper runup model was reported by Sielecki and Wurtele (1970)<sup>90</sup>. They employed three different finite difference techniques, among them the Lax-Wendroff method, for the NLSW equations with the Coriolis term. A simple extrapolation combined with an asymmetric representation was used to follow the shoreline. Among the test cases were  $CG-i^5$ , that was well reproduced except for a small discrepancy at shoreline, and a three-dimensional eigenoscillation in a parabolic basin<sup>100</sup> that was simulated perfectly. In 1975 Flather and Heaps<sup>13</sup> published a 3D FD technique for the NLSW equations, based on the C-grid, with a scheme to update wet and dry regions. However, the model was applied to tidal oscillations in a bay without any verification of its runup performance. Hibberd and Peregrine (1979)<sup>27</sup> employed the Lax-Wendroff technique to the NLSW equations in conservative form and obtained a model for non-breaking waves as well as bores. According to the authors the simple shoreline method of Sielecki and Wurtele<sup>90</sup> did not suffice for these problems. After attempting various methods they settled for a predictor-corrector sequence of linear extrapolations and applications of the physical equations in the vicinity of the shoreline. Even though some near-shore deviations were identified, both  $CG-i^5$  and  $CG-s^5$  were reproduced well. Very close agreement were reported with analytical runup heights<sup>67</sup>, while the theoretical values overshoot measurements<sup>69</sup>. This was explained by viscous effects that must influence the thin swash zone significantly on laboratory scale. Later Kobayashi (1987)<sup>46</sup> adopted the method and applied it to runup on rough slopes.

Kowalik and Murty (1993)<sup>47</sup> employed linear onshore extrapolation of velocity and surface elevation with a C-grid discretization of the NLSW equations. Their method gave reasonably good results for  $CG-i^5$  and the first mode in a parabolic basin, but with significant noise at the shoreline. Then they used the method to compute the inundation in a real tsunami event.

With the experiments on solitary wave runup on a conical island Briggs *et al.* (1995)<sup>2</sup> (Sec. 3.3) provided what still is the only 3D dataset well suited for verification of models. In a companion paper Liu *et al.*<sup>52</sup> presented NLSW simulations with a C-grid model with upwind representation

of the convective terms. The moving shoreline was represented through a sequence of over-toppings and dry-outs in a step-bathymetry. In spite of some deviation the maximum runup heights were generally predicted very well for the smaller amplitudes. Moreover, even though the sharp local maximum at the lee side was not fully reproduced for  $A/d = 0.1$ , the nonlinear model fared much better than linear solutions<sup>14,38</sup> in this respect. Recently, the same method was re-applied to this case for  $A/d = 0.1$ , utilizing a hierarchical grid to obtain selective grid-refinement around the island<sup>10</sup>. However, no substantial improvement was obtained. The results of Liu *et al.* for the highest amplitude were less good. According to the discussion in Sec. 3.3, this case really requires a dispersive model. At the time the only well documented Boussinesq type model for three-dimensional runup was the Lagrangian method of Zelt and Raichlen<sup>115</sup>, described in Sec. 4.1. Regretfully, to the knowledge of the author this finite element model is never applied to the conical island problem.

Titov and Synolakis (1995)<sup>101</sup> used the characteristic form of the 2D NLSW equations that were solved by a corrected leap-frog method allowing for non-uniform grids. This enabled the inclusion of an auxiliary shoreline point in the otherwise fixed grid. The position and velocity for the extra point were projected from the nearest wet point. Good agreement with experiments<sup>94</sup> and the formula (17) was obtained for non-breaking solitary wave runup. The method also gave rather good agreement with experiments on a breaking wave ( $A/d = 0.3$ ), save for some pronounced deviation in the early phase of runup. However, this may partly be due to the sensitivity of the solutions to small time differences at this stage (Sec. 3.2), but omission of dispersion did probably contribute as well. Later the method was generalized to three dimensions by operator splitting<sup>102</sup>. Comparison was then made to the conical island experiment<sup>2</sup> with very good agreement for  $A/d = 0.1$  and somewhat larger errors for  $A/d = 0.2$ . The latter may again be due to the absence of dispersion. Physical tsunami applications displayed encouraging results indeed and demonstrated that the method is robust in complex situations and handles features as merging of shorelines. It is incorporated in the tsunami model known as MOST<sup>73</sup>.

Madsen *et al.*<sup>62</sup> reported a 3D Boussinesq technique with improved linear dispersion characteristics, based on depth integrated volume fluxes, and a surface roller model for breaking. The beach was made slightly permeable with a porosity, rapidly decreasing from unity to a small residual value beneath the surface. As a consequence the equations could be solved throughout a region that was extended beyond the shoreline, with no explicit

reference to its position. However, as communicated by the authors, this technique was not without weaknesses. The dispersion terms was turned off in the onshore motion, noise had to filtered and there was a mass deficit in the swash tongue due to the porosity. The latter caused marked deviations from the  $CG-s^5$  solution, while the overall agreement was still reasonably good. Subsequently, the porous shore technique were amended and incorporated in the FUNWAVE model<sup>45</sup> for improved Boussinesq equations (Sec. 2.6), with results presented in a series of papers. In a paper on rip-currents Chen *et al.* (1999)<sup>8</sup> interpreted the porosity as slots in the seabed and counterbalanced the volume loss by adjusting the inter-slot beach level. Wave breaking was represented by an eddy viscosity depending on the temporal surface gradient (Sec. 2.5). This model was put to test by Kennedy *et al.* (2000)<sup>42</sup> through comparison with experiments on breaking in finite depth and the analytic  $CG-s^5$  solution. The model reproduced the breaking well, while the agreement with  $CG-s^5$  was substantially improved relative to Madsen *et al.*<sup>62</sup>, even if some deviation persisted. Chen *et al.* (2000)<sup>9</sup> did the conical island test. The agreement for the smaller amplitudes,  $A/d = 0.05, 0.1$  was fairly good, but poorer rather than better relative to the pre-existing NLSW computations<sup>52,102</sup>. For the higher amplitude,  $A/d = 0.2$ , where dispersion is more important, the results improved, at least compared to Liu *et al.* (1995)<sup>52</sup>. Unfortunately, simulations based on the porous bed technique appeared not to have been compared to the detailed experimental surface profiles for breaking and non-breaking waves<sup>94</sup>.

The runup facility in the COULWAVE model<sup>56</sup> for the improved Boussinesq equations was described and tested in Lynett *et al.* (2002)<sup>57</sup>. Again wet and dry nodes were recognized by the total water depth, while the discrete equations at the shoreline were based systematically on fictitious nodes beyond the shoreline. Linear extrapolation from neighboring points in the fluid was used to assign values to the onshore nodes. Higher order differences were then used throughout the computational domain. In principle, this is a simple procedure that may seem to depend heavily on the analytic nature of the solution. The authors presented a good description of the implications of the procedure for the computational molecules adjacent to the shore. In addition to the general loss of accuracy and noise (arrested by a 9 point filter) at the shoreline, the higher order spatial derivatives were annihilated, which imply omission of dispersion terms. Wave breaking was included in a similar manner as in Kennedy *et al.* (2000)<sup>42</sup>. Model results agreed well with  $CG-s^5$  and the second eigenmode in a parabolic basin<sup>100</sup>

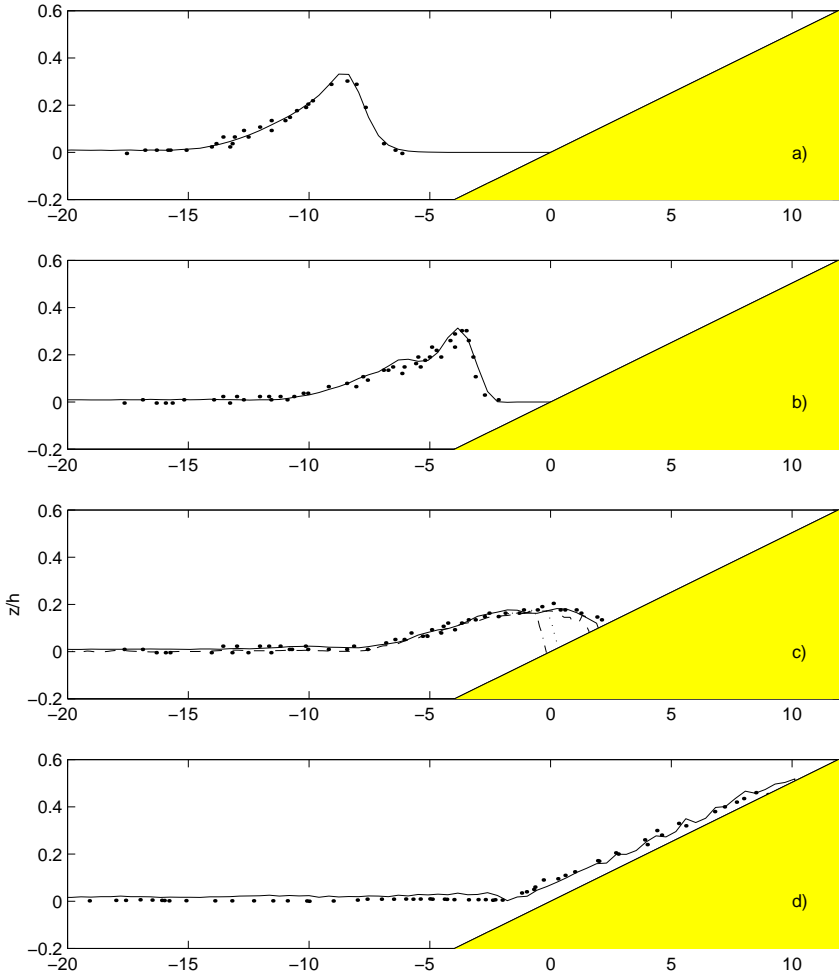


Fig. 10. Breaking solitary wave runup. Experiments from Synolakis<sup>94</sup> are indicated by markers, while the fully drawn lines are solutions from Lynett *et al.*<sup>57</sup>. Panel (c) includes also results from Zelt<sup>114</sup> (dots), Titov and Synolakis<sup>101</sup> (dash-dot) and the N-S computations of Lin *et al.*<sup>51</sup> (dashes). Reproduced from Lynett *et al.* by courtesy of the Coastal Engineering.

was accurately reproduced. Also the conical island test was made with good results. For runup of a breaking wave ( $A/d = 0.3$ ) impressive agreement was obtained with both experiments<sup>94</sup> and a turbulent Navier-Stokes simulation<sup>51</sup> (Fig. 10). Even though this is unlikely to be the reason for the good outcome, it must be noted that the choice of the coefficient in the

bottom-drag was optimized. As pointed out by the authors, there are still some unresolved shortcomings in the model for features like over-topping and reentry of a runup tongue into quiescent water<sup>56</sup>.

Another line of runup modeling is based on the NLSW equations in conservative form, finite volume techniques and approximate Riemann solvers to include bores as sharp jumps in the solution. This branch will be covered in depth in Chapter 2 in this volume by LeVeque and George<sup>48</sup>. Hence, we refer briefly only a selection of contributions, with emphasis on runup tests. The shoreline may be treated by the special Riemann problem related to penetration of gas into vacuum or dam-break. However, this leads to overestimation of the pressure gradient and acceleration at the shoreline. Hence, modelers often resort to complete or partial exclusion of very shallow cells from the general computation scheme. The flux and source terms in the momentum equation (see below Eq. (6)) are generally separated by operator splitting, even though Watson *et al.* (1992)<sup>106</sup> suggested the inclusion of the source term in the Riemann problem by a local transformation to an accelerating frame of reference. Sleigh *et al.* (1998)<sup>91</sup> invoked a discretization into triangular volumes which enables flexible local grid refinement. The method was tested on various dam-break problems and bore-runup. Good agreement was observed with the analytical solution for the standard dam-break problem, save from small deviations at the toe. Two-dimensional simulations were presented by Hu *et al.* (2000)<sup>30</sup> including runup of non-breaking solitary waves, that agreed closely with an analytic solution<sup>94</sup>, and the standard dam-break problem. The latter case demonstrated that exemption of shallow cells provide a better solution near the fluid tip than application of a modified Riemann solution. In Brocchini *et al.* (2001)<sup>3</sup> operator splitting was employed on a rectangular grid and a Riemann technique was used for the shoreline. Results compare well with the analytic solution  $CG-i^5$  and the standard dam-break problem. However, for the latter there was noticeable spurious behavior close to the water line. The particular strength of Hubbard and Dodd (2002)<sup>31</sup> is a hierarchical mesh refinement, which means that finer rectangular grids may be superimposed on coarser ones in regions that require high resolution, as the shore and swash zone. Close agreement, save for small irregularities at the shore, was obtained with  $CG-s^5$ . Surprisingly, the reproduction of the first nonlinear eigenmode in a parabolic basin was less good.

A common objective for this kind of models is to preserve sharp bore fronts. It would have been interesting to see a detailed comparison with real, finite width bores, as breaking solitary waves<sup>94</sup>.

The finite element method has a much weaker merit in Eulerian runup modeling than the finite difference counterpart. Several methods for including a moving shoreline in a static FE grid have been proposed<sup>105</sup>, but few have been validated by comparison to reference solutions or systematic grid refinement. An interesting attempt on solving a two-dimensional Boussinesq equation with the differentiable Hermitian cubic shape functions was made by Gopalakrishnan and Tung (1983)<sup>18</sup>. The pressure gradient was used directly to compute the shoreline acceleration which then was integrated to yield the position. The shore element was then modified at each time step, and split/deleted when appropriate. However, the only application was solitary wave runup, without any comparison to other solutions nor application of grid refinement tests. Moreover, the presented solutions clearly displayed noise and spurious features. Later the method was modified<sup>17</sup> to the three-dimensional NLSW equations and applied to tidal flooding, again with inadequate testing of the runup performance. Umetsu (1995)<sup>104</sup> employed partially dry triangular elements, where the velocities on dry near-shore nodes are imposed as averages of the values from the adjacent wet ones. The technique performed well for broken dam flow, but produced outspoken deviation from the  $CG-i^5$ , in particular close to the shore. In Takagi (1996)<sup>98</sup> the technique was applied to the conical island problem with reasonably good, but not convincing, result.

## 5. Discussion

The crucial point in runup modeling is the representation of the shoreline motion, for which the presence of a singularity (Sec. 2.4) calls for caution. The literature refer many rather crude as well as sophisticated methods for the moving boundary. Even though noise in the vicinity of the shoreline is often observed there are few severe problems that have been attributed to the singularity. It is tempting to assume that this problem is not that grave after all, or that a logarithmic singularity is too weak to be fatal. On the other hand, too many authors have treated numerical convergence rather loosely. More rigid grid refinement studies might reveal that there indeed are irregularities at the shore, even though they in most applications will be overshadowed by other error sources. Anyway, the bottom line is that there is a diversity of working runup models about.

The recent progress in long wave runup modeling may roughly be divided into two directions: one where the runup facility is integrated in general purpose wave propagation models with high order inherent dispersion

and another where increasingly robust or accurate shoreline representations are included in NLSW models, with features like adaptive grids and shock capturing. Some of the NLSW models are both well tested, efficient, and flexible enough for, for instance, realistic case studies of tsunami, while the existing Boussinesq type models still may miss a little on runup/drawdown, bore presentation and computer efficiency for such applications. On the other hand, dispersion is important for wave propagation in finite depth, not only for swells, but also for many tsunamis. This leads to the questions; when are the different kind of long wave models appropriate and how may they be combined in applications that require the strengths of both kind of models?

Our little study of significance of dispersion, reflected in Fig. 5, suggests that the NLSW equations may be very accurate for the near-shore region and runup for non-breaking waves. Regretfully, it is difficult to attain further insight on this point from the literature. Truly, in some of the cases of non-breaking solitary wave runup, reviewed in the previous section, the inclusion of dispersion led to improved agreement with experiments or more general models<sup>57,114</sup>. However, the difference may be due to accumulation of dispersion effects in finite depth propagation and shoaling (Sec. 3.1) that change the incident wave before the shoreline is reached, and that are missed out in the NLSW solution. For the case of breaking solitary wave runup<sup>94</sup> the improved Boussinesq solution<sup>57</sup> is clearly superior to those of the NLSW<sup>101</sup> and standard Boussinesq equations<sup>114</sup> (Fig. 10). Still, again the effect of dispersion on the incident presumably is important. In addition the bore representation are very different in the respective models, and even somewhat dubious for the standard Boussinesq formulation in question. Hence, it is difficult to draw any firm conclusion on the local near-shore effect of non-hydrostatic pressure and more investigations are required, where local effects are emphasized.

If, for a given application, the dispersion can be neglected near-shore, but not elsewhere, nesting of models may be desirable. For instance, a higher order Boussinesq type description for deep water propagation and shoaling should be coupled with an efficient NLSW solver with shock handling and robust runup properties for the surf and swash regions. A one way coupling from Boussinesq to NLSW equations is principally straightforward. On the other hand, a two way coupling involves conceptual problems. The NLSW solver will produce and preserve shocks sharp, except at the shoreline. In finite depths the shocks may vanish only due to dissipation. Hence, the reflected waves from shallow region may be difficult to convey to a

Boussinesq type model without severe problems. To the knowledge of the author no such attempt on a complete two way coupling has been reported in the literature.

For Lagrangian, and curvilinear, models very good performance is reported for runup of waves in 2D or simple 3D geometries. This makes transformed domain models an excellent tool for academic studies. However, a widely accepted weakness of such methods is the strong grid deformation that may occur in demanding applications. No well documented attempt to apply such models to real tsunami studies has been reported. In fact, in recent years Lagrangian coordinates, in general, have been most popular in connection with smooth particle hydrodynamics that is a meshless method. It would have been interesting to see how well such a method could be employed with the NLSW equations and free boundaries.

### Acknowledgments

The author wishes to thank Professor P. L.-F. Liu and Professor P. Lynett for their helpful assistance.

### References

1. A. Balzano. Evaluation of methods for numerical simulation of wetting and drying in shallow water flow models. *Coast. Eng.* **34**, 83–107 (1998).
2. M. J. Briggs, C. E. Synolakis, G. S. Harkins and D. R. Green. Laboratory experiments of tsunami runup on circular island. *Pure and Applied Geophysics* **144**(3/4), 569–593 (1995).
3. M. Brocchini, R. Bernetti, A. Mancinelli and G. Albertini. An efficient solver for nearshore flows based on the WAF method. *Coast. Eng.* **43**, 105–129 (2001).
4. G. F. Carrier. Gravity waves on water of variable depth. *J. Fluid Mech.* **24**, 641–659 (1966).
5. G. F. Carrier and H. P. Greenspan. Water waves of finite amplitude on a sloping beach. *J. Fluid Mech.* **4**, 97–109 (1958).
6. G. F. Carrier, T. T. Wu and H. Yeh. Tsunami run-up and draw-down on a plane beach. *J. Fluid Mech.* **475**, 79–99 (2003).
7. Y. Chen and P. L.-F. Liu. Modified Boussinesq equations and associated parabolic models for water wave propagation. *J. Fluid Mech.* **288**, 351–381 (1995).
8. Q. Chen, R. A. Dalrymple, J. T. Kirby, A. B. Kennedy and M. C. Haller. Boussinesq modeling of a rip current system. *J. Geophys. Res.* **104**, 20617–20637 (1999).
9. Q. Chen, J. T. Kirby, R. A. Dalrymple, A. B. Kennedy and A. Chawla. Boussinesq modeling of wave transformation, breaking, and run-up. Part II: 2D. *J. Waterw., Port, Coast., Ocean Engrg.* **126**(1), 48–56 (2000).

10. Y.-S. Cho, K.-Y. Park and T.-H. Lin. Run-up heights of nearshore tsunamis based on quadtree grid system. *Ocean engineering* **31**, 1093–1109 (2004).
11. E. D. Cokelet. Breaking waves. *Nature* **267**, 769–774 (1977).
12. B. Elfrink and T. Baldock. Hydrodynamics and sediment transport in the swash zone: a review and perspectives. *Coastal Engineering* **45**, 149–167 (2002).
13. R. A. Flather and N. S. Heaps. Tidal computations for Morecambe Bay. *Geophys. J.R. Astr. Soc.* **42**, 489–517 (1975).
14. K. Fujima. Application of linear theory to the computation of runup of solitary waves on a conical island. In *Long-wave runup models*, Eds. H. Yeh, C. E. Synolakis and P. L.-F. Liu (World Scientific Publishing Co., 1996), p. 221–230.
15. B. Gjevik and G. Pedersen. Run-up of long waves on an inclined plane. Preprint series in applied mathematics, Dept. of Mathematics, University of Oslo (1981).
16. M. F. Gobbi, J. T. Kirby and G. Wei. A fully nonlinear Boussinesq model for surface waves. Part 2. Extension to  $O(kh)^4$ . *J. Fluid Mech.* **405**, 181–210 (2000).
17. T. C. Gopalakrishnan. A moving boundary circulation model for regions with large tidal flats. *Int. J. Num. Meth. Eng.* **28**, 245–260 (1989).
18. T. C. Gopalakrishnan and C. C. Tung. Numerical analysis of a moving boundary problem in coastal hydrodynamics. *Int. J. Num. Meth. Fluids* **3**, 179–200 (1983).
19. D. G. Goring. Tsunamis: The propagation of long waves onto a shelf. Ph.D. thesis Rep. KH-R-38, Calif. Inst. Technol., Pasadena, California (2003).
20. C. Goto. Nonlinear equations of long waves in the Lagrangian description. *Coast. Eng. Japan* **22**, 1–9 (1979).
21. C. Goto and N. Shuto. Run-up of tsunamis by linear and nonlinear theories. In *Coastal Engineering. Proc. of the seventeenth Coastal Engineering Conf., vol. 1* (Sydney, Australia, 1980), p. 695–70.
22. C. Goto and N. Shuto, Numerical simulation of tsunami propagations and run-up. In *Tsunamis—Their Science and Engineering*, Eds. K. Lida and T. Iwasaki (TERRAPUB, 1983), p. 439–451.
23. S. Grilli and I. A. Svendsen. Computation of nonlinear wave kinematics during propagation and run-up on a slope. In *Water wave kinematics* (Kluwer Academic Publishers, 1990), p. 378–412.
24. S. T. Grilli, I. A. Svendsen and R. Subramanya. Breaking criterion and characteristics for solitary waves on slopes. *J. Waterw., Port, Coast., Ocean Engrg.* (1997).
25. S. Guignard, R. Marcer, V. Rey, K. Kharif and Fraunié. Solitary wave breaking on sloping beaches; 2-D two phase flow numerical simulation by SL-VOF method. *Eur. J. Mech. B-Fluids* **20**, 57–74 (2001).
26. J. V. Hall and J. W. Watts. Laboratory investigation of the vertical rise of solitary waves on impermeable slopes. Tech. Memo. 33, Beach Erosion Board, U.S. Army Corps of Engrs. (1953).

27. S. Hibberd and D. H. Peregrine. Surf and run-up on a beach: a uniform bore. *J. Fluid Mech* **95**, 323–345 (1979).
28. D. V. Ho, R. E. Meyer and M. C. Chen. Long surf. *J. Mar. Res.* **21**, 219–232 (1963).
29. S.-H. Hsiao, P. L.-F. Liu and Y. Chen. Nonlinear water waves propagating over a permeable bed. *Phil. Trans. R. Soc. Lond. A* **458**, 1291–1322 (2002).
30. K. Hu, C. G. Mingham and D. M. Causon. Numerical simulation of wave overtopping of coastal structures using the non-linear shallow water equations. *Coast. Eng.* **41**, 433–465 (2000).
31. M. E. Hubbard and N. Dodd. A 2D numerical model of wave run-up and overtopping. *Coast. Eng.* **47**, 1–26 (2002).
32. F. Imamura. Review of tsunami simulation with a finite difference method. In *Long-wave runup models*, Eds. H. Yeh, C. E. Synolakis and P. L.-F. Liu (World Scientific Publishing Co., 1996), p. 25–42.
33. E. Isaacson. Water waves over a sloping bottom. *Comm. Pure Appl. Math* **3**, 11–31 (1950).
34. A. Jensen, G. Pedersen and D. J. Wood. An experimental study of wave run-up at a steep beach. *J. Fluid. Mech.* **486**, 161–188 (2003).
35. B. Johns. Numerical integration of the shallow water equations over a sloping shelf. *Int. J. Numer. Methods Fluids* **2**, 253–261 (1982).
36. H. Johnsgard. A numerical model for run-up of breaking waves. *Int. J. Num. Meth. Fluids* **31**, 1321–1331 (1999).
37. H. Johnsgard and G. Pedersen. A numerical model for three-dimensional run-up. *Int. J. Num. Meth. Fluids* **24**, 913–931 (1997).
38. U. K anoğlu and C. E. Synolakis, Analytic solutions of solitary wave runup on the conical island and on the reverse beach. In *Long-wave runup models*, Eds. H. Yeh, C. E. Synolakis and P. L.-F. Liu (World Scientific Publishing Co., 1996), p. 215–220.
39. U. K anoğlu and C. E. Synolakis. Long wave runup on piecewise linear topographies. *J. Fluid Mech.* **374**, 1–28 (1998).
40. T. Kataoka and M. Tsutahara. Transverse instability of surface solitary waves. *J. Fluid Mech.* **512**, 211–221 (2004).
41. H. B. Keller, A. D. Levine and G. B. Whitham. Motion of a bore over a sloping beach. *J. Fluid Mech.* **7**, 302–316 (1960).
42. A. B. Kennedy, Q. Chen, J. T. Kirby and R. A. Dalrymple. Boussinesq modeling of wave transformation, breaking, and run-up. Part I: 1D. *J. Waterw., Port, Coast., Ocean Engrg.* **126**(1), 39–47 (2000).
43. S. K. Kim, P. L.-F. Liu and J. A. Liggett. Boundary integral solutions for solitary wave generation, propagation and run-up. *Coast. Eng.* **7**, 299–317 (1983).
44. J. T. Kirby. Funwave software download page (1998).  
**URL:** <http://chinacat.coastal.udel.edu>.
45. J. T. Kirby, G. Wei, , Q. Chen, A. B. Kennedy and R. A. Dalrymple. Fully nonlinear Boussinesq wave model documentation and user’s manual. Research Report CACR-98-06, Center for applied Coastal research, Department of Civil Engineering, University of Delaware, Newark, DE 19716,

September 1998.

**URL:** <http://chinacat.coastal.udel.edu>.

46. N. Kobayashi, A. K. Otta and I. Roy. Wave reflection and run-up on rough slopes. *J. Waterw., Port, Coast., Ocean Engrg. Div. ASCE*. **113**, 282–298 (1987).
47. Z. Kowalik and T. S. Murty. Numerical simulation of two-dimensional tsunami run-up. *Marine Geodesy* **16**, 87–100 (1993).
48. R. J. LeVeque and D. L. George. High-resolution finite volume methods for the shallow water equations with bathymetry and dry states. In *Advanced Numerical Models for Simulating Tsunami Waves and Runup*, eds. P. L.-F. Liu, H. Yeh and C. Synolakis (World Scientific Publishing Co., 2008), p. 43–73.
49. Y. Li and F. Raichlen. Solitary wave runup on plane slopes. *J. Waterw., Port, Coast., Ocean Engrg.* **127**(1), 33–44 (2001).
50. Y. Li and F. Raichlen. Non-breaking and breaking solitary wave run-up. *J. Fluid Mech.* **456**, 295–318 (2002).
51. Pengzhi Lin, Kuang-An Chang and Philip L.-F. Liu. Runup and rundown of solitary waves on sloping beaches. *J. Waterw., Port, Coast., Ocean Engrg.* **125**(5), 247–255 (1999).
52. P. L.-F. Liu, Y.-S. Cho, M. J. Briggs, U. Kânoğlu and C. E. Synolakis. Runup of solitary waves on a circular island. *J. Fluid Mech.* **302**, 259–285 (1995).
53. P. L.-F. Liu, C. E. Synolakis and H. Yeh. Report on the international workshop on long-wave run-up. *J. Fluid Mech.* **229**, 675–688 (1991).
54. S. Longo, M. Petti and I. J. Losada. Turbulence in the swash and surf zones: a review. *Coastal Engineering* **45**, 129–147 (2002).
55. D. R. Lynch and W. G. Gray. Finite element simulation of flow in deforming regions. *J. Comp. Phys.* **36**, 135–153 (1980).
56. P. J. Lynett and P. L.-F. Liu. Coulwave model page (2004).  
**URL:** <http://ceprofs.tamu.edu/plynett/COULWAVE/default.htm>.
57. P. J. Lynett, T.-R. Wu and P. L.-F. Liu. Modeling wave runup with depth-integrated equations. *Coast. Eng.* **46**, 89–107 (2002).
58. P. A. Madsen, H. B. Bingham and H. Liu. A new Boussinesq method for fully nonlinear waves from shallow to deep water. *J. Fluid Mech.* **462**, 1–30 (2002).
59. P. A. Madsen, R. Murray and O. R. Sørensen. A new form of the Boussinesq equations with improved linear dispersion characteristics. *Coast. Eng.* **15**, 371–388 (1991).
60. P. A. Madsen and H. A. Schäffer. Higher-order Boussinesq-type equations for surface gravity waves: derivation and analysis. *Phil. Trans. R. Soc. Lond. A* **356**, 3123–3184 (1998).
61. P. A. Madsen and H. A. Schäffer. A review of Boussinesq-type equations for surface gravity waves. *Advances in Coastal and Ocean Engineering, vol. 5* (World Scientific Publishing Co., 1999), p. 1–95.

62. P. A. Madsen, O. R. Sørensen and H. A. Schäffer. Surf zone dynamics simulated by a Boussinesq-type model: Part I. model description and cross-shore motion of regular waves. *Coast. Eng.* **32**, 255–287 (1997).
63. J. C. Martin, W. J. Moyce, W. G. Penney, A. T. Price and C. K. Thornhill. Some gravity wave problems in the motion of perfect liquids. *Philosophical Transactions of Royal Society of London, Ser. A* **244**, 231–334 (1952).
64. F. Mesinger and A. Arakawa. Numerical methods used in atmospheric models. *GARP, Publ. Ser. WMO* **17**, (1976).
65. R. E. Meyer. On the shore singularity of water wave theory. Part 1. The local model. *Physics of Fluids* **19**, 3142–3163 (1986).
66. R. E. Meyer. On the shore singularity of water wave theory. Part 2. Small waves do not break on gentle beaches. *Physics of Fluids* **19**, 3164–3171 (1986).
67. R. E. Meyer and A. D. Taylor. Run-up on beaches. In *Waves on Beaches and Resulting Sediment Transport* (Academic Press, 1972) p. 357–411.
68. J. W. Miles. Solitary waves. *Ann. Rev. Fluid Mech.* **12**, 11–43 (1980).
69. R. L. Miller. Experimental determination of run-up of undular and fully developed bores. *J. Geophys. Res.* **73**, 4497–4510 (1968).
70. J. J. Monaghan and A. Kos. Solitary waves on a Cretan beach. *J. Waterw., Port, Coast., Ocean Engrg.* **125**(3), 145–154 (1999).
71. O. Nwogu. Alternative form of Boussinesq equations for nearshore wave propagation. *J. Waterw., Port, Coast., Ocean Engrg.* **119**(6), 618–638 (1993).
72. H. T. Özkan-Haller and J. T. Kirby. A Fourier-Chebyshev collocation method for the shallow water equations including shoreline run-up. *Applied Ocean Research* **19**, 21–34 (1997).
73. Pacific Marine Environmental Laboratory. Tsunami Research Program (2005),  
**URL:** <http://www.pmel.noaa.gov/tsunami/research.html>.
74. G. Pedersen. Run-up of periodic waves on a straight beach. Preprint Series in Applied Mathematics, ISBN 82-553-0952-7 1/85, Dept. of Mathematics, University of Oslo, Norway (1985).
75. G. Pedersen and B. Gjevik. Run-up of solitary waves. *J. Fluid Mech.* **135**, 283–299 (1983).
76. G. Pedersen. A Lagrangian model applied to runup problems. In *Advanced Numerical Models for Simulating Tsunami Waves and Runup*, eds. P. L.-F. Liu, H. Yeh and C. Synolakis (World Scientific Publishing Co., 2008), p. 311–315.
77. E. Pelinovsky, O. Kozyrev and E. Troshina. Tsunami runup in a sloping channel. In *Long-wave runup models*, Eds. H. Yeh, C. E. Synolakis and P. L.-F. Liu (World Scientific Publishing Co., 1996), p. 332–339.
78. D. H. Peregrine. Long waves on a beach. *J. Fluid Mech.* **77**, 417–431 (1967).
79. D. H. Peregrine. Equations for water waves and the approximation behind them. In *Waves on beaches*, Ed. E. Meyer (Academic Press, New York, 1972), p. 357–412.
80. D. H. Peregrine. Breaking waves on beaches. *Ann. rev. of Fluid Mech.* **15**, 149–178 (1983).

81. D. H. Peregrine and S. M. Williams. Swash overtopping a truncated plane beach. *J. Fluid Mech.* **440**, 391–399 (2001).
82. J. Petera and V. Nassehi. A new two-dimensional finite element model for the shallow water equations using a Lagrangian framework constructed along fluid particle trajectories. *Int. J. Num. Meth. in Eng.* **39**, 4159–4182 (1996).
83. M. Petti and S. Longo. Turbulence experiments in the swash zone. *Coastal Engineering* **43**, 1–24 (2001).
84. R. S. Prasad and I. A. Svendsen. Moving shoreline boundary condition for nearshore models. *Coast. Eng.* **49**(4), 239–261 (2003).
85. J. A. Puleo, R. A. Beach, R. A. Holman and J. S. Allen. Swash zone sediment suspension and transport and the importance of bore-generated turbulence. *J. Geophys. Res.* **105**(C7), 17021–17044 (2000).
86. R. O. Reid and B. R. Bodine. Numerical model for storm surges in Galveston Bay. *J. Waterw., Port, Coast., Ocean Engrg. Div. ASCE* **94**(WW1), 33–57 (1968).
87. M. C. Shen and R. E. Meyer. Climb of a bore on a beach **3**, run-up. *J. Fluid Mech.* **16**, 113–125 (1963).
88. F. Shi and W. Sun. A variable boundary model of storm surge flooding in generalized curvilinear grids. *Int. J. Numer. Methods Fluids* **21**, 641–651 (1995).
89. N. Shuto. Run-up of long waves on a sloping beach. *Coastal Engng. in Japan* **10**, 23–38 (1967).
90. A. Sielecki and M. G. Wurtele. The numerical integration of the nonlinear shallow-water equations with sloping boundaries. *J. Comp. Phys.* **6**, 219–236 (1970).
91. P. A. Sleigh, P. H. Gaskell, M. Berszins and N. G. Wright. An unstructured finite-volume algorithm for predicting flow in rivers and estuaries. *Computers & Fluids* **27**(4), 479–508 (1998).
92. L. Q. Spielvogel. Single wave run-up on sloping beaches. *J. Fluid Mech.* **74**, 685–694 (1976).
93. J.J. Stoker. *Water waves*. (Interscience, 1957).
94. C. E. Synolakis. The run-up of solitary waves. *J. Fluid Mech.* **185**, 523–545 (1987).
95. C. E. Synolakis, M. K. Deb and J. E. Skjelbreia. The anomalous behaviour of the run-up of cnoidal waves. *Phys. Fluids* **31**, 3–5 (1988).
96. C. E. Synolakis and J. E. Skjelbreia. Evolution of maximum amplitude of solitary waves on plane beaches. *J. Waterw., Port, Coast., Ocean Engrg.* **119**(3), 323–342 (1993).
97. S. Tadepalli and C. Synolakis. The run-up of N-waves on sloping beaches. *Proc. R. Soc. Lond. A* **445**, 99–112 (1994).
98. T. Takagi. Finite element analysis in bench mark problems 2 and 3. In *Long-wave runup models*, Eds. H. Yeh, C. E. Synolakis and P. L.-F. Liu (World Scientific Publishing Co., 1996), p. 258–264.
99. H. Takeda. Numerical simulation of run-up by variable transformation. *J. of the Oceanographical Society of Japan* **40**, 271–278 (1984).

100. W. C. Thacker. Some exact solutions to the nonlinear shallow-water wave equations. *J. Fluid Mech.* **107**, 499–508 (1981).
101. V. V. Titov and C. E. Synolakis. Modeling of breaking and nonbreaking long-wave evolution and runup using VTCS-2. *J. Waterw., Port, Coast., Ocean Engrg.* **121**(6), 308–316 (1995).
102. V. V. Titov and C. E. Synolakis. Numerical modeling of tidal wave runup. *J. Waterw., Port, Coast., Ocean Engrg.* **124**(4), 157–171 (1998).
103. E. O. Tuck and L.-S. Hwang. Long wave generation on a sloping beach. *J. Fluid Mech.* **51**(3), 449–461 (1972).
104. T. Umetsu. A boundary condition technique of moving boundary simulation for broken dam problem by three-step explicit finite element method. In *Advances in Hydro-Science and Engineering, Vol. II*, (Tsinghua University Press, Beijing, 1995), p. 394–399.
105. A. Walters and T. Takagi. Review of finite element methods for tsunami simulations. In *Long-wave runup models*, Eds. H. Yeh, C. E. Synolakis and P. L.-F. Liu (World Scientific Publishing Co., 1996), p. 43–87.
106. G. Watson, D. H. Peregrine and E. F. Toro. Numerical solution of the shallow water equations on a beach using the weighted average flux method. In *Computational Fluid Dynamics '92* Eds. Ch. Hirsch, J. Pèriaux and W. Kordulla (Elsevier Science Publishers, 1992), p. 495–502.
107. G. Wei, J. T. Kirby, S. T. Grilli and R. Subramanya. A fully nonlinear Boussinesq model for surface waves. Part 1. Highly nonlinear unsteady waves. *J. Fluid Mech.* **294**, 71–92 (1995).
108. J.-K. Woo and P. L.-F. Liu. Finite element model for modified Boussinesq equations. I: Model development. *J. Waterw., Port, Coast., Ocean Engrg.* **130**(1), 1–16 (2004).
109. D.J. Wood, G. Pedersen and A. Jensen. Modelling of run-up of steep non-breaking waves. *Ocean Engineering* **30**, 625–644 (2003).
110. T. Y. Wu. Long waves in ocean and coastal waters. *Proc. ASCE, J. Eng. Mech. Div.* **107**, 501–522 (1981).
111. H. Yeh, A. Ghazali and I. Marton. Experimental study of a bore run-up. *J. Fluid Mech.* **206**, 563–578 (1989).
112. H. Yeh, P. L.-F. Liu, M. Briggs and C. E. Synolakis. Propagation and amplification of tsunamis at coastal boundaries. *Nature* **372**, 353–355 (1994).
113. H. Yeh, C. E. Synolakis and P. L.-F. Liu, Eds., *Long-wave runup models*. (World Scientific Publishing Co., 1996).
114. J. A. Zelt. The run-up of nonbreaking and breaking solitary waves. *Coast. Eng.* **15**, 205–246 (1991).
115. J. A. Zelt and F. Raichlen. A Lagrangian model for wave-induced harbour oscillations. *J. Fluid Mech.* **213**, 203–225 (1990).
116. J. A. Zelt and F. Raichlen. Overland flow from solitary waves. *J. Waterw., Port, Coast., Ocean Engrg.* **117**, 247–263 (1991).
117. X. Zhou, Y. C. Hon and K. F. Cheung. A grid-free, nonlinear shallow-water model with moving boundary. *Engineering Analysis with Boundary Elements* **28**(8), 967–973 (2004).